

# ChemComm

Accepted Manuscript



This article can be cited before page numbers have been issued, to do this please use: Z. Wang, J. Liu, Y. Fu, C. Liu, Z. Liu, C. Pan and G. Yu, *Chem. Commun.*, 2017, DOI: 10.1039/C7CC00704C.



This is an Accepted Manuscript, which has been through the Royal Society of Chemistry peer review process and has been accepted for publication.

Accepted Manuscripts are published online shortly after acceptance, before technical editing, formatting and proof reading. Using this free service, authors can make their results available to the community, in citable form, before we publish the edited article. We will replace this Accepted Manuscript with the edited and formatted Advance Article as soon as it is available.

You can find more information about Accepted Manuscripts in the [author guidelines](#).

Please note that technical editing may introduce minor changes to the text and/or graphics, which may alter content. The journal's standard [Terms & Conditions](#) and the ethical guidelines, outlined in our [author and reviewer resource centre](#), still apply. In no event shall the Royal Society of Chemistry be held responsible for any errors or omissions in this Accepted Manuscript or any consequences arising from the use of any information it contains.



Journal Name

COMMUNICATION

## Fabrication of Conjugated Microporous Polytriazine Nanotubes and Nanospheres for Highly Selective CO<sub>2</sub> capture

Zhiqiang Wang,<sup>†a,b</sup> Junling Liu,<sup>†b</sup> Yu Fu,<sup>b</sup> Cheng Liu,<sup>c</sup> Chunyue Pan,<sup>b</sup> Zhiyong Liu,<sup>a,\*</sup> and Guipeng Yu<sup>b,\*</sup>Received 00th January 20xx,  
Accepted 00th January 20xx

DOI: 10.1039/x0xx00000x

www.rsc.org/

**Abstract:** A one-spot template approach for fabricating porous organic nanotubes was developed and a molecular design, i.e. introducing thiophene and s-triazine functionality to enhance host-guest interactions led to novel porous solids with high capacities for CO<sub>2</sub> and exceptionally high ideal selectivities over N<sub>2</sub> for effective gas storage and separation.

Covalently linked nanoporous organic polymers (NOPs) have attracted increasing interests for their excellent physicochemical properties and promising potential in gas storage<sup>1</sup>, separation<sup>2</sup>, electronics<sup>3</sup> and biosensors<sup>4</sup>. From the viewpoint of the material synthesis, NOPs—due to their functional diversity—combine flexible design and synthetic diversity, and are a growing platform for such applications<sup>5,6</sup>. As for synthetic strategies, a kaleidoscope of organic reactions namely condensation of aromatic diboronic acids<sup>7</sup>, ionothermal reaction<sup>8</sup>, Suzuki cross-coupling reaction<sup>9</sup>, and Yamamoto-type Ullmann coupling reaction<sup>10</sup> have been successfully employed. Purely organic nanoporous mainly micro-/meso-porous materials as well as their construction technology are however still a contemporary field of materials chemistry.

For an ideal sorbent materials with good absorption capability, high pore volume, large specific surface area, and suitable adsorption enthalpy and morphology<sup>11</sup> are essential. To achieve this goal, topological combination of the building units with different geometries and sizes have been used to change the skeletons and pores of the materials. Up to now, most research efforts have been paid to improve the specific surface area<sup>12</sup> and host-guest interaction<sup>13</sup> and to adjust pore size<sup>14</sup>. While more recently reducing the size of NOPs to nanometer scale has attracted continuously increasing attention. As for the morphology of NOPs,

most frequent forms are aggregated microspheres<sup>15</sup>. Also, there are a small amount of layered sheets<sup>16</sup>, core-shell<sup>17</sup>, jagged morphologies<sup>18</sup> and irregular shapes<sup>19</sup>. Tubular NOPs are very rare due to the lack of proper synthetic protocols and remain highly desired not only for their fascinating tubular nanostructure which provides access to three different contact regions (inner, outer surfaces and ends) but also for good flexibility in functionalization as well as sufficient understanding of the morphology-physical property relationships. Deng *et al.* have reported nanotube-like CMPs and their great potentials for separation of organic solvents and oils from water<sup>20</sup> and also demonstrated the significant impact of reaction mediums on morphologies of as-made CMPs<sup>21</sup>. Son disclosed the tubular-shape evolution of amorphous MONs prepared by Sonogashira coupling between tetrahedral multialkyne and dihalo building blocks.<sup>22</sup> Notably, nanocarbons-templated method has been developed for the construction of microporous networks with well-defined nanotube morphologies<sup>23</sup>. The convenient, simple operation and easy-handling methods for the production of morphology-controllable NOPs remains an aspect that need to more contribution to insight into.

It has been proven that introduction of electron-rich aromatic rings and heteroatoms such as nitrogen<sup>24</sup> can significantly improve host-guest interaction of NOPs and their performance as a porous medium for the storage of small gases. Thiophene, as an electron-rich aromatic ring containing sulfur, is one of the most popular and well-established building units acting as an electron donor in organic conductive polymers while is rarely used for the construction of NOPs. Herein, we attempted to develop an undisclosed thiophene-based conjugated microporous polymer (termed as CMP-CSU13) featuring good affinity towards CO<sub>2</sub> and significantly high selectivity of CO<sub>2</sub> against nitrogen (Fig. 1). We also demonstrate a facile *in-situ* template approach for fabricating tubular meso-/micro-porous networks with controlled dimensions under mild conditions.

In this regard, the thiophene moiety was successfully introduced into the porous polymer backbone using a popular grown method used to obtain Porous Aromatic Frameworks<sup>6</sup>. Starting from a triangular monomer namely 2,4,6-tris(5-bromothiophen-2-yl)-1,3,5-triazine (TBPT), the targeted CMP-CSU13 (Fig.1a) were readily obtained.

<sup>a</sup> College of Chemistry and Chemical Engineering, Key Laboratory for Chemical Materials of Xinjiang Uygur Autonomous Region/Engineering Center for Chemical Materials of Xinjiang Corps, Shihezi University, Xinjiang, Shihezi 832003, China. E-mail: lzyongclin@sina.com.

<sup>b</sup> College of Chemistry and Chemical Engineering, Central South University, Changsha 410083, China. E-mail: gilbertyu@csu.edu.cn.

<sup>c</sup> State key Laboratory of Fine Chemicals, Dalian University of Technology, Dalian 110762, China.

<sup>†</sup> These authors contributed equally to this work.

Electronic Supplementary Information (ESI) available: [Materials, Characterization Methods and results, Synthesis procedures, etc.]. See DOI: 10.1039/x0xx00000x

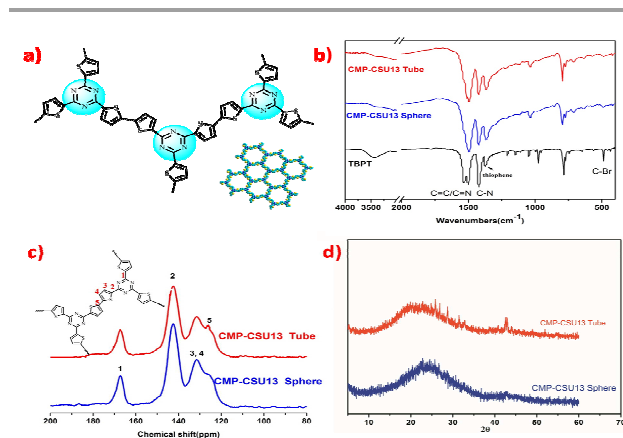


Fig. 1 (a) Chemical structure and illustration, (b) FT-IR spectrum, (c)  $^{13}\text{C}/\text{MAS}$  NMR spectrum, (d) PXRD patterns of CMP-CSU13 tube (Red) and sphere (Blue).

ned through Nickel (0)-catalyzed Yamamoto-type Ullmann coupling which was known as an aryl-aryl coupling of aryl-halogenide compounds mediated mostly by bis(1,5-cyclooctadiene)nickel(0) with a proposed mechanism (Fig. S1, ESI $^{\dagger}$ )<sup>25</sup>. Under such conditions, our halogenide TBPT demonstrated an unexpected halogen elimination ability, making the development of ultrahigh porosity polymers easily accessible. Therefore, high-degree-crosslinking networks with abundant thiophene units were successfully obtained in decent yields (exceeding 71 %).

Our strategy for preparing porous nanotubes is rather simple, and the idea was inspired by the nanocarbon-templated method<sup>23</sup> and also rod-shaped structure and the high surface-energy of nanocrystals<sup>26</sup>. Given the fact this Yamamoto-type Ullmann coupling polymerization was usually performed in dimethylformide (DMF) with 2,2'-bipyridyl as an acid acceptor, it is proposed that the nanocrystals, i.e. quaternary ammonium salts can be easily formed *in-situ* by the quaternisation of 2,2'-bipyridyl with suitable halogenide compounds (Fig. 2). In this way, the tubular polymers may be accessed by using such nanocrystals as structurally directing templates. While in such reaction conditions, we failed to directly convert our aromatic halogenide compound (TBPT) to a quaternary ammonium salt because of its low reactivity towards 2,2'-bipyridyl, regardless of the potential great difficulty in further growing of nanocrystals. 1,2-dibromoethane was chosen as a key additive in our polymerization system to ensure the formation of ammonium salts nanocrystals. At the polymerization temperatures, the charge of 1,2-dibromoethane readily converted part of 2,2'-bipyridyl into its water-soluble ammonium salt, which was precipitated out and then the expected nanometer-sized rod-like crystals were formed as confirmed by transmission electron microscopy (TEM, Fig. S2, ESI $^{\dagger}$ ). Next, with the growing length of nanocrystals along their axes, the crosslinking of polymers was carried out on the surfaces of the nanocrystals, and thus, core/shell structures may be formed. With the proceeding of the polymerization, oligomers like rigid dendrimers or macrocycles were produced in the early stage, and they were easily adhered onto the template surface due to the high surface-energy of the nanocrystals. In the last purification step, the nanocrystals inside the cavity of the products were easily removed by washing with concentrated hydrochloric acid and water. In the

continuous search for synthetic conditions for purely tubular materials, equivalent amount of 1,2-dibromoethane plus [Ni(cod)<sub>2</sub>] against 2,2'-bipyridyl is a dominant factor for reliable generation of tubular networks. Varying the molar content of 1,2-dibromoethane and 2,2'-bipyridyl and their concentrations, the size of the nanocrystals can be well controlled, leading to tubular porous networks with tunable dimensions. For comparison, 0D ball-like CMP (CMP-CSU13 sphere) was also prepared by the same procedure without the addition of 1,2-dibromoethane.

The structure of TBPT (Scheme S1) was confirmed by spectral measurements (Fig.S3-4, ESI $^{\dagger}$ ). The CMP-CSU13 obtained are insoluble in all organic solvents and also chemically stable in dilute solutions of acids and bases. Differential scanning calorimetry (Fig. S5, ESI $^{\dagger}$ ) and thermo gravimetric analysis (Fig.S6, ESI $^{\dagger}$ ) demonstrate their good thermal stability. The residual weight (around 1 % under air atmosphere) at 800 °C, may be scripted to the presence of nickel oxide and silicon oxide generated by oxidation of residual catalyst, well agreeing with EDS mapping result (Fig. S7, ESI $^{\dagger}$ ).

FT-IR (Fig. 1b) and  $^{13}\text{C}/\text{MAS}$  NMR spectra (Fig.1c) of tubular and ball-like CMP-CSU13 matched well with the expected structure. The tested element contents by Element Analysis show a slight deviation (Table. S1, ESI $^{\dagger}$ ), which may be reasonable considering that trace amount of cocatalyst like 2,2'-bipyridyl trapped in the pores even after an overnight Soxhlet extraction. PXRD patterns indicate both the tubular and ball-like samples are amorphous (Fig. 1d). A careful comparison of the FT-IR,  $^{13}\text{C}/\text{MAS}$  NMR and PXRD patterns suggests that there is no clear difference between the tubular samples and spheres ones. These prove that the incorporation of *in-situ* generated nanocrystal templates did not affect the polymerization reaction significantly.

In order to probe morphology texture of CMP-CSU13, scanning electron microscopy (SEM) and TEM measurements were carried out. It is clear from SEM images that the tubes are uniform noodle-like fibers entangled with each other (Fig. 3a). Typically, the tubes are several micrometers in length. Most of them have an outer diameter of about 80–160 nm and a length of about 1-5  $\mu\text{m}$ , depending on the molar content of 1,2-dibromoethane and 2,2'-bipyridyl and also their concentrations in the reaction medium (Table S2, Fig. S8-10, ESI $^{\dagger}$ ). Our results demonstrated an significant increase on outer diameter of the nanotubes with the increasing molar content of 1,2-dibromoethane and 2,2'-bipyridyl in the polymerization system. Within a dilute polymerization system (Entry 5), the majority of as-made nanotubes possess a decreased diameter and length of  $90\pm 10$  nm and 1-4 $\mu\text{m}$ , respectively. Notably,

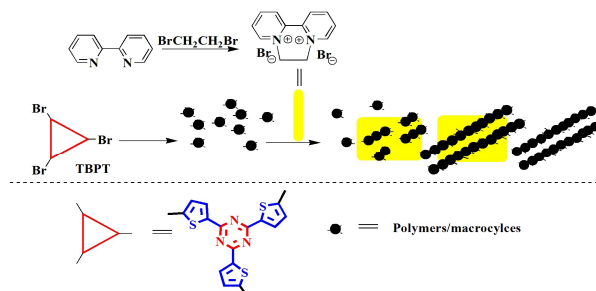


Fig. 2 Suggested mechanistic aspects of free-standing tubular CMP-CSU13

the surfaces of the tubes are covered by spherical tubercles featuring a diameter of about 10–30 nm, as shown in Fig. 2a. The TEM images (Fig. 2b and 2c) reveal that the resultant networks possess hollow tubular structures, further confirming the success of *in-situ* template method. In contrast, without the addition of 1,2-dibromoethane in the polymerization system (Entry 0-1, Table S2, ESI<sup>†</sup>), only nanospheres accompanying with larger fused masses were observed (Fig. 2d). Further evidence comes from the TEM visualizations (Fig. 2e, 2f) in which the majority of the nanospheres with a diameter of about 100–200 nm were demonstrated. Notably, in our investigated range the diameter of the porous shells could easily be adjusted by varying the BFPT/solvent medium ratio (Table S2, ESI<sup>†</sup>). Surface Gibbs free energy was probably the dominant driving force to form CMP nanospheres in our system. Therefore, it is reasonable considering the fact that the spherical structure has the lowest surface Gibbs free energy compared with other morphologies. High resolution TEM (HR-TEM) images exhibit alternating dark and bright areas, insinuating a porous structure of the resulting networks. To exclude the possibility that the nanotube evolution in morphology was solely caused by the dispersion of the solvents or self-assembly after polymerization, four kinds of solvents with different polarity, i.e. *n*-hexane (Permittivity=1.9), ethanol (24.5), acetone (20.7) and water (78.5) were used to disperse the resulting samples. A careful comparison of HR-TEM demonstrated that the nanotubes or aggregated microsphere morphology just depends on the exact polymerization conditions,

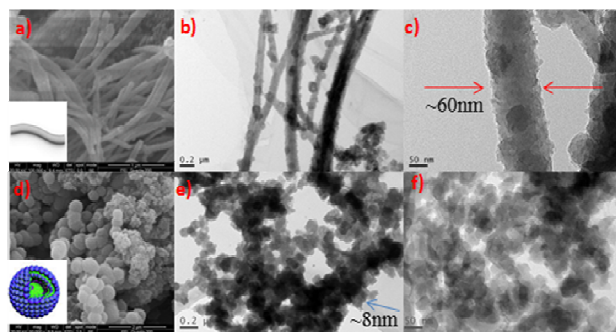


Fig. 3 SEM image (a), TEM image (b), HR-TEM image (c) of tubular CMP-CSU13; SEM image (d), TEM image (e), HR-TEM image (f) of ball-like CMP-CSU13

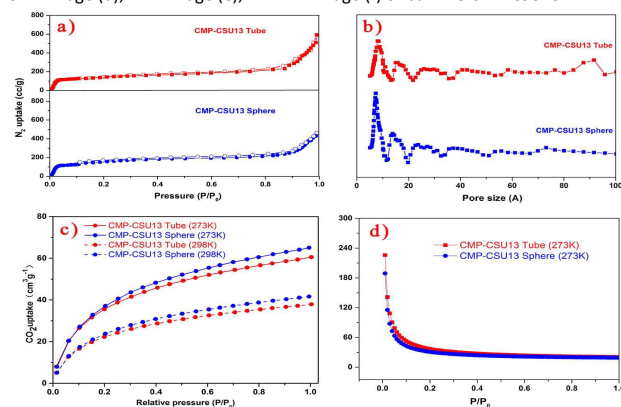


Fig. 4 (a)  $N_2$  adsorption isotherms, (b) Pore size distributions by DFT method, (c)  $CO_2$  adsorption isotherms, (d) IAST ideal selectivities of CMP-CSU13 tube (Red) and sphere (Blue).

while there is no clear relationship with the nature of dispersion solvents (Fig. S11, ESI<sup>†</sup>). Permanent porosity of the CMP-CSU13 pair was confirmed by  $N_2$  adsorption/desorption isotherms (Fig. 4a). The isotherms are Type I, albeit with a very modest micropore step and some Type IV character. The BET surface area calculated was  $741 \text{ m}^2 \text{ g}^{-1}$  for the tubular samples and this value is still comparable to those reported for CMPs ( $200\text{--}900 \text{ m}^2 \text{ g}^{-1}$ ) from similar aromatic building blocks. Both CMP-CSU13 tubes and spheres show large total pore volumes up to  $1.07 \text{ cc g}^{-1}$ , which is far larger than the famous CMPs with even higher surface areas<sup>3,24</sup> (Tab. S3, ESI<sup>†</sup>). It is suggesting that the incorporation of thiophene into the backbone and the aryl-aryl coupling chemistry would effectively prevent the collapse of the nanopores.

Unlike reported procedures<sup>23b</sup>, our results indicate that employing the nanocrystall templates in the preparation procedures will not affect the pore structure of the as-made CMPs. Pore size distribution (PSD), as shown in Fig. 4b, was analyzed by a with Non-local density functional theory (NLDFT), and the pores in CMP-CSU13 are widely distributed, from micropore to mesopore, in particular, mainly located in the range of 0.5 to 10 nm with dominant pores centered at 0.6 and 1.4 nm, indicative of a hierarchal pore nature (Fig. S14–15, ESI<sup>†</sup>). Tubular sample possesses a wider pore size distribution with typical mesoporosity expanded to 8.2 nm, while these samples with different morphologies display some similarities in the PSD curves, implying their similar topology.

$CO_2$  sorption property was investigated by volumetric method at 273 and 298 K (Fig. 4c, Fig. S16, ESI<sup>†</sup>). A slightly higher  $CO_2$  uptake capacity is attained by CMP-CSU13 nanosphere in comparison with tubular one under same conditions, attributed to its larger pore volume and easier diffusion of guest gases in the sphere morphology. This implies that the morphology of the sorbents exerts a significant effect for the low-pressure  $CO_2$  storage, and the adsorption behaviour depends less on the surface area than that in the high pressures. Compared to the reported CMPs, our CMP-CSU13 exhibits the highest capacity although delivering a moderate surface area. Such high capacities are also comparable to other NOPs such as binaphthol-based HCPs (17.4 wt% at 1 bar and 273 K)<sup>11</sup> and triazine-based CTF-0 (15.7 wt% at 1 bar and 273 K)<sup>8a</sup>.

The isosteric enthalpies of adsorption ( $Q_{st}$ ) were calculated by Clausius-Clapeyron equation on the basis of the  $CO_2$  isotherms recorded at 273 K and 298 K. The  $Q_{st}$  values at a low coverage are arranged in the following decreasing sequence (Fig. S17, ESI<sup>†</sup>): CMP-CSU13 nanotube ( $40.3 \text{ kJ mol}^{-1}$ ) > CMP-CSU13 nanosphere ( $36.2 \text{ kJ mol}^{-1}$ ). Both the samples deliver significantly high  $Q_{st}$  values ( $>35 \text{ kJ mol}^{-1}$ ) for  $CO_2$  adsorption, surpassing those of other porous organic polymers like CMP-1, PAF-1 ( $15.6 \text{ kJ/mol}$ )<sup>27</sup> and BILPs<sup>28</sup>. This may be reasonable, considering the fact that the resultant networks with abundant nitrogen or electro-rich thiophene units intrinsically favour  $CO_2$  and contribute to the enhanced performance, because of the promoted dipole-quadrupole interaction.

The selective adsorption of  $CO_2$  over  $N_2$  is critical for carbon capture from air or flue gas streams. Ideal selectivity of  $CO_2$  over  $N_2$  was calculated at an equilibrium partial pressure of 85 wt%  $N_2$  and 15 wt%  $CO_2$  in the bulk phase using IAST model<sup>29</sup>. The synthesized CMP-CSU13 pairs deliver significantly high selectivities (Fig. 4d, Fig. S18–21, ESI<sup>†</sup>). The tubular CMP-CSU13 possesses an unexceptionally high ideal selectivity of  $CO_2$ -over- $N_2$  of 223 at zero coverage, being

## COMMUNICATION

Journal Name

slightly larger than its sphere counterpart, while to the best of our knowledge this value is sufficiently superior to those of most NOPs like CTF-0 and binaphthol-based HCPs<sup>11</sup>. It may be reasonable considering the abundant narrow ultramicropores (<1 nm) and the presence of electron-rich thiophene rings makes a significant contribution to CO<sub>2</sub> adsorption at low loadings, considering thermodynamic size of CO<sub>2</sub>. Thus, these materials would hold considerable promise for post-combustion carbon capture applications.

In summary, we have successfully synthesized a tubular porous organic polymer (CMP-CSU13) via an *in-situ* template approach. This strategy was quite convenient in terms of handling and separation and was applicable to other multiply halogenate monomers, which was significant in preparing functional CMP tubes on a large scale. As an added bonus, the resultant networks have demonstrated an unusual large total pore volume together with high adsorption enthalpies for CO<sub>2</sub> (up to 40.3 kJ/mol). Moreover, such thiophene-functional nitrogen-rich networks feature possessed exceptionally high IAST ideal selectivities over nitrogen (up to 223 at 273 K) at low CO<sub>2</sub> loading, which make them promising sorbents for gas separations. Given the universality of building blocks in chemistry and the structural diversity of CMPs, we expect this work could also provide a new route for developing dispersible and uniform functional CMPs with controllable morphology.

## Acknowledgements

We acknowledge the financial support from the National Science Foundation of China (Nos. 51662036, 21674129, 21376272 and 21636010), State Key Laboratory of Fine Chemicals (KF1604) and Joint Funds of Hunan Provincial Natural Science Foundation and ZhuZhou Municipal Government of China (2015JJ5010).

## Notes and references

- H. Jiang, D. Feng, T. Liu, J. Li and H. Zhou, *J. Am. Chem. Soc.*, 2012, **134**, 14690.
- N. B. McKeown and P. M. Budd, *Chem. Soc. Rev.*, 2006, **35**, 675.
- J. X. Jiang, F. B. Su, A. Trewin, C. D. Wood, H. J. Niu, J. T. A. Jones, Y. Z. Khimyak and A. I. Cooper, *J. Am. Chem. Soc.*, 2008, **130**, 7710.
- X. Liu, Y. Xu, D. Jiang, *J. Am. Chem. Soc.* 2012, **134**, 8738.
- T. Ben, H. Ren, S. Ma, D. Cao, J. Lan, X. Jing, W. Wang, J. Xu, F. Deng, J. M. Simmons, S. Qiu and G. Zhu, *Angew Chem Int Ed*, 2009, **48**, 9457.
- N. B. McKeown, B. Gahnem, K. J. Msayib, P. M. Budd, C. E. Tattershall, K. Mahmood, S. Tan, D. Book, H. W. Langmi and A. Walton, *Angew. Chem. Int. Ed.*, 2006, **45**, 1804.
- C. J. Doonan, D. J. Tranchemontagne, T. G. Glover, J. R. Hunt and O. M. Yaghi, *Nat. Chem.*, 2010, **2**, 235.
- (a) P. Katekomol, J. Roeser, M. Bojdys, J. Weber and A. Thomas, *Chem. Mater.*, 2013, **25**, 1542. (b) S. Wu, Y. Liu, G. Yu, C. Pan, Y. Du, X. Xiong and Z. Wang, *Macromolecules*, 2014, **47**, 2875. (c) K. Yuan, C. Liu, J. Han, G. Yu, J. Wang, H. Duan, Z. Wang and X. Jian, *RSC Adv.*, 2016, **6**, 12009.
- Q. Chen, M. Luo, T. Wang, J. Wang, D. Zhou, Y. Han, C. Zhang, C. Yan and B. Han, *Macromolecules*, 2011, **44**, 5573.
- C. Zhang, Y. Liu, B. Li, B. Tan, C. Chen, H. Xu and X. Yang, *ACS Macro. Lett.*, 2011, **1**, 190.
- R. Dawson, L. A. Stevens, T. C. Drage, C. E. Snape, M. W. Smith, D. J. Adams and A. I. Cooper, *J. Am. Chem. Soc.*, 2012, **134**, 10741.
- (a) O. Plietzsch, C. I. Schilling, T. Grab, S. L. Grage, A. S. Ulrich, A. Comotti, P. Sozzani, T. Muller and S. Bräse, *New J. Chem.*, 2011, **35**, 1577. (b) Y. Liu, S. Wu, G. Wang, G. Yu, J. Guan, C. Pan and Z. Wang, *J. Mater. Chem. A*, 2014, **2**, 7795. (c) D. Y. Chen, S. Gu, Y. Fu, Y. L. Zhu, C. Liu, G. H. Li, G. P. Yu and C. Y. Pan, *Polym. Chem.*, 2016, **7**, 3416.
- (a) M. G. R. T. Karl T. Jackson, *Polym. Chem.*, 2011, 2775. (b) L. Pan, Q. Chen, J. H. Zhu, J. G. Yu, Y. J. He and B. H. Han, *Polym. Chem.*, 2015, **6**, 2478. (c) X. Fu, Y. Zhang, S. Gu, Y. Zhu, G. Yu, C. Pan, Y. Hu, *Chem.-A Euro. J.*, 2015, **21**, 13357.
- (a) X. Feng, L. Chen, Y. Dong and D. Jiang, *Chem Commun*, 2011, **47**, 1979. (b) M. R. Liebl and J. R. Senker, *Chem. Mater.*, 2013, **25**, 970. (c) C. Y. Pei, T. Ben, Y. Q. Li and S. L. Qiu, *Chem. Commun.*, 2014, **50**, 6134.
- (a) H. Yu, C. Shen, M. Tian, J. Qu and Z. Wang, *Macromolecules*, 2012, **45**, 5140. (b) O. G. Rabbani and A. H. M. El-Kader, *Chem. Mater.*, 2012, 1511.
- Z. Xiang and D. Cao, *Macromol. Rapid. Commun.*, 2012, **33**, 1184.
- Y. Xu, A. Nagai and D. L. Jiang, *Chem. Commun.*, 2013, **49**, 1591.
- M. Dogru, A. Sonnauer, A. Gavryushin, P. Knochel and T. Bein, *Chem. Commun.*, 2011, **47**, 1707.
- S. Wan, J. Guo, J. Kim, H. Ihee and D. Jiang, *Angew. Chem. Int. Ed.*, 2008, **47**, 8826.
- A. Li, H. Sun, D. Tan, W. Fan, S. Wen, X. Qing, G. Li, S. Li and W. Deng, *Energ. Environ. Sci.*, 2011, **4**, 2062.
- D. Tan, W. Xiong, H. Sun, Z. Zhang, W. Ma, C. Meng, W. Fan and A. Li, *Micropor. Mesopor. Mat.*, 2013.
- N. Kang, J. H. Park, J. Choi, J. Jin, J. Chun, I. G. Jung and S. U. Son, *Angew. Chem. Int. Ed.*, 2012, **51**, 6626.
- (a) X. Zhuang, D. Gehrig, N. Forler, H. Liang, M. Wagner, M. R. Hansen, F. Zhang and X. Feng, *Adv. Mater.*, 2015, **27**, 3789. (b) M. G. Schwab, D. Crespy, X. Feng, K. Landfester and K. Müllen, *Macromol. Rapid Commun.*, 2011, **32**, 1798.
- (a) X. Zhu, C. Tian, S. M. Mahurin, S. Chai, C. Wang, S. Brown, G. M. Veith, H. Luo, H. Liu and S. Dai, *J. Am. Chem. Soc.*, 2012, **134**, 10478. (b) S. Ren, R. Dawson, A. Laybourn, J. Jiang, Y. Khimyak, D. J. Adams and A. I. Cooper, *Polym. Chem.*, 2012, **3**, 928. (c) S. Gu, J. He, Y. Zhu, Z. Wang, D. Chen, G. Yu, J. Guan and K. Tao, *ACS Appl. Mater. Inter.*, 2016, **8**, 18383.
- T. Yamamoto, *Bull. Chem. Soc. Jpn.*, 1999, **72**, 621.
- L. Zhu, Y. Xu, W. Yuan, J. Xi, X. Huang, X. Tang, and S. Zheng, *Adv. Mater.*, 2006, **18**, 2997.
- Y. Xu, S. Jin, H. Xu, A. Nagai and D. Jiang, *Chem. Soc. Rev.*, 2013, **42**, 8012.
- W. Zhao, Z. Hou, Z. Yao, X. Zhuang, F. Zhang and X. Feng, *Polym. Chem.*, 2015, **6**, 7171.
- M. R. Liebl and J. R. Senker, *Chem. Mater.*, 2013, **25**, 970-980.